

# BIJECTIVE PROOFS FOR SCHUR FUNCTION IDENTITIES

MARKUS FULMEK

ABSTRACT. In [4], Gurevich, Pyatov and Saponov stated an expansion for the product of two Schur functions and gave a proof based on the Plücker relations.

Here we show that this identity is in fact a special case of a quite general Schur function identity, which was stated and proved in [1, Lemma 16]. In [1], it was used to prove bijectively Dodgson’s condensation formula and the Plücker relations, but was not paid further attention: So we take this opportunity to make obvious the range of applicability of this identity by giving concrete examples, accompanied by many graphical illustrations.

## 1. INTRODUCTION

In [4], Gurevich, Pyatov and Saponov stated an expansion for the product of two Schur functions and gave a proof based on the Plücker relations. Here we show that this identity is in fact a special case of a more general Schur function identity [1, Lemma 16]. Since this involves a process of “translation” between the languages of [1] and [4] which might not be self-evident, we explain again the corresponding combinatorial constructions here. These constructions are best conceived by pictures, so we give a lot of figures illustrating the concepts.

This paper is organized as follows:

In Section 2 we recall the basic definitions (partitions, Young tableaux, skew Schur functions and nonintersecting lattice paths).

In Section 3, we present the central bijective construction (recolouring of bicoloured paths in the overlays of families of nonintersecting lattice paths corresponding to some product of skew Schur functions) and show how this yields a quite general Schur function identity (Theorem 1, a reformulation of [1, Lemma 16]).

In Section 4 we try to exhibit the broad range of applications of Theorem 1: In particular, we show how the identity [4, (3.3)] appears as (a translation of) a special case of Theorem 1.

## 2. BASIC DEFINITIONS

An infinite weakly decreasing series of nonnegative integers  $(\lambda_i)_{i=1}^{\infty}$ , where only finitely many elements are positive, is called a *partition*. The largest index  $i$  for which  $\lambda_i > 0$  is

---

*Date:* September 29, 2009.

Research supported by the National Research Network “Analytic Combinatorics and Probabilistic Number Theory”, funded by the Austrian Science Foundation.

called the *length* of the partition  $\lambda$  and is denoted by  $\ell(\lambda)$ . For convenience, we shall in most cases omit the trailing zeroes, i.e., for  $\ell(\lambda) = r$  we simply write  $\lambda = (\lambda_1, \lambda_2, \dots, \lambda_r)$ , where  $\lambda_1 \geq \lambda_2 \geq \dots \geq \lambda_r > 0$ .

The *Ferrers diagram*  $F_\lambda$  of  $\lambda$  is an array of cells with  $\ell(\lambda)$  left-justified rows and  $\lambda_i$  cells in row  $i$ .

An  $N$ -*semistandard Young tableau* of shape  $\lambda$  is a filling of the cells of  $F_\lambda$  with integers from the set  $\{1, 2, \dots, N\}$ , such that the numbers filled into the cells weakly increase in rows and strictly increase in columns.

Let  $T$  be a semistandard Young tableau and define  $m(T, k)$  to be the number of entries  $k$  in  $T$ . Then the weight  $w(T)$  of  $T$  is defined as follows:

$$\omega(T) = \prod_{k=1}^N x_k^{m(T,k)}.$$

*Schur functions*, which are irreducible general linear characters, can be combinatorially defined by means of  $N$ -semistandard Young tableaux (see, for instance, [5, Definition 4.4.1]):

$$s_\lambda(x_1, x_2, x_3, \dots, x_N) = \sum_T \omega(T),$$

where the sum is over all  $N$ -semistandard Young tableaux  $T$  of shape  $\lambda$ .

Consider some partition  $\lambda = (\lambda_1, \dots, \lambda_r > 0)$ , and let  $\mu$  be a partition such that  $\mu_i \leq \lambda_i$  for all  $i \geq 1$ . The *skew Ferrers diagram*  $F_{\lambda/\mu}$  of  $\lambda/\mu$  is an array of cells with  $r$  left-justified rows and  $\lambda_i - \mu_i$  cells in row  $i$ , where the first  $\mu_i$  cells in row  $i$  are missing. An  $N$ -*semistandard skew Young tableau* of shape  $\lambda/\mu$  is a filling of the cells of  $F_{\lambda/\mu}$  with integers from the set  $\{1, 2, \dots, N\}$ , such that the numbers filled into the cells weakly increase in rows and strictly increase in columns (see the left picture of Figure 1 for an illustration).

Then we can define the *skew Schur function*:

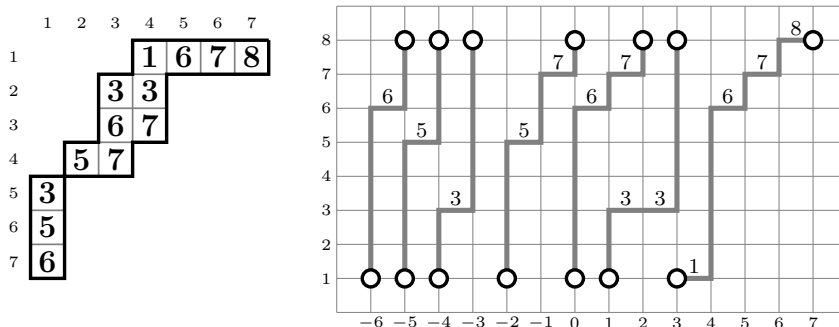
$$s_{\lambda/\mu}(x_1, x_2, x_3, \dots, x_N) = \sum_T \omega(T), \tag{1}$$

where the sum is over all  $N$ -semistandard skew Young tableaux  $T$  of shape  $\lambda/\mu$ , where the weight  $\omega(T)$  of  $T$  is defined as before.

Note that for  $\mu = (0, 0, \dots)$  the skew Schur function  $s_{\lambda/\mu}$  is identical to the ‘‘ordinary’’ Schur function  $s_\lambda$ .

The Gessel-Viennot interpretation [2] gives an equivalent description of a semistandard Young tableau  $T$  of shape  $\lambda/\mu$  as an  $r$ -tuple  $P = (p_1, \dots, p_r)$  of nonintersecting lattice paths, where  $r := \ell(\lambda)$ : Fix some (arbitrary) integer *shift*  $t$  and consider paths in the lattice  $\mathbb{Z}^2$  (i.e., in the directed graph with vertices  $\mathbb{Z} \times \mathbb{Z}$  and arcs from  $(j, k)$  to  $(j+1, k)$  and from  $(j, k)$  to  $(j, k+1)$  for all  $j, k$ ). The  $i$ -th path  $p_i$  starts at  $(\mu_i - i + t, 1)$  and ends at  $(\lambda_i - i + t, N)$ , and the  $j$ -th *horizontal* step in  $p_i$  goes from  $(-i + t + j - 1, h)$

FIGURE 1. The left picture presents a semistandard Young tableau  $T$  of skew shape  $\lambda/\mu$ , where  $\lambda = (7, 4, 4, 3, 1, 1, 1)$  and  $\mu = (3, 2, 2, 1)$ . Assuming that the entries of  $T$  are chosen from  $\{1, 2, \dots, 8\}$  (i.e.:  $T$  is an 8-semistandard Young tableau), the right picture shows the corresponding family of  $7 = \ell(\lambda)$  nonintersecting lattice paths (with shift  $t = 0$ ): Note that the height of the  $j$ -th horizontal step in the  $i$ -th path (the paths are counted from right to left) is equal to the  $j$ -th entry in row  $i$  of  $T$ .



to  $(-i + t + j, h)$ , where  $h$  is the  $j$ -th entry in row  $i$  of  $T$ . Note that the conditions on the entries of  $T$  imply that no two paths  $p_i$  and  $p_j$  thus defined have a lattice point in common: such an  $r$ -tuple of paths is called *nonintersecting* (see the right picture of Figure 1 for an illustration).

In fact, this translation of tableaux to nonintersecting lattice paths is a *bijection* between the set of all  $N$ -semistandard Young tableaux of shape  $\lambda/\mu$  and the set of all  $r$ -tuples of nonintersecting lattice paths with starting and ending points as defined above. This bijection is *weight preserving* if we define the weight of an  $r$ -tuple  $P$  of nonintersecting lattice paths in the obvious way, i.e., as

$$\omega(P) := \prod_{k=1}^N x_k^{n(P,k)},$$

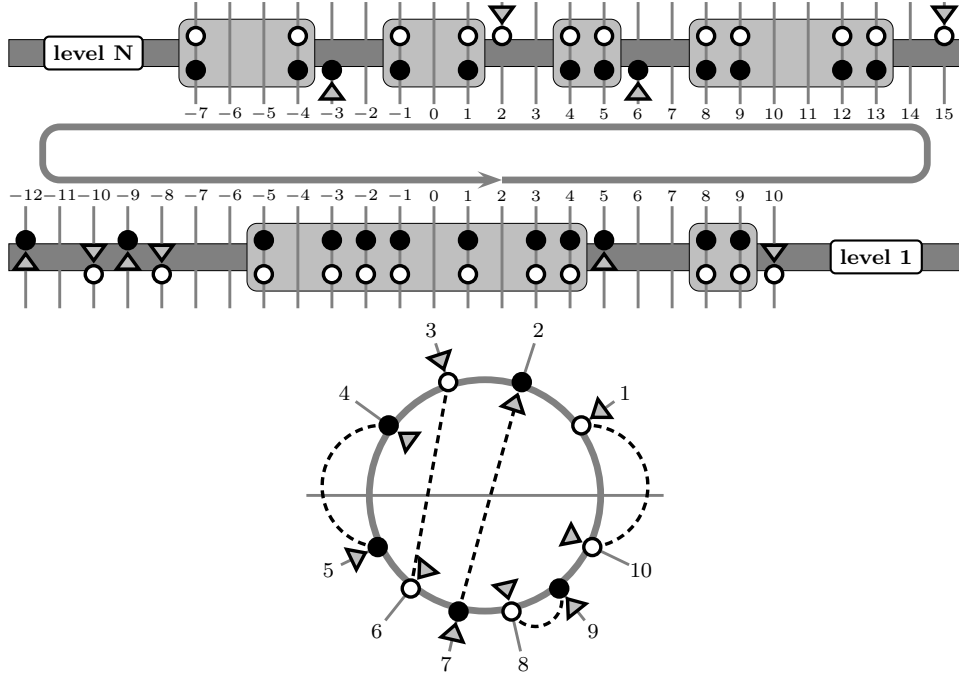
where  $n(P, k)$  is the number of horizontal steps at height  $k$  in  $P$ . So in the definition (1) we could equivalently replace symbol “ $T$ ” by symbol “ $P$ ”, and sum over  $r$ -tuples of lattice paths with prescribed starting and ending points instead of tableaux with prescribed shape.

Note that the horizontal coordinates of starting and ending points determine uniquely the *shape*  $\lambda/\mu$  of the tableau, and the vertical coordinate (we shall call the vertical coordinate of points the *level* in the following) of the ending points determines uniquely the *set of entries*  $\{1, 2, \dots, N\}$  of the tableau. (The choice of the shift parameter  $t$  does influence neither the shape nor the set of entries.)

### 3. BICOLOURED PATHS AND PRODUCTS OF SKEW SCHUR FUNCTIONS

In the following, all skew Schur functions are considered as functions of the variables  $(x_1, \dots, x_N)$ . (Equivalently, all tableaux have entries from the set  $\{1, \dots, N\}$ , and all families of nonintersecting lattice paths have ending points on level  $N$ ).

FIGURE 2. Illustration for the example given in Section 3.



Viewing the product of two skew Schur functions

$$s_{\lambda/\mu} \cdot s_{\sigma/\tau}$$

as the generating function of “overlays of two families of nonintersecting lattice paths” (according to definition (1)) gives rise to a bijective construction, which (to the best of our knowledge) was first used by Goulden [3]. This construction was used in [1] to describe and prove a class of Schur function identities, special cases of which imply Dodgson’s condensation formula and the Plücker relations.

We shall present this construction by way of an example: Consider skew shapes  $\lambda/\mu$ , where

$$\begin{aligned} \lambda &= (14, 13, 13, 11, 11, 9, 9, 8, 8, 7, 5, 3), \\ \mu &= (9, 9, 9, 6, 6, 5, 4, 4, 4, 3, 1), \end{aligned} \tag{2}$$

and  $\sigma/\tau$ , where

$$\begin{aligned} \sigma &= (14, 14, 12, 12, 11, 11, 11, 9, 8, 7, 7, 5), \\ \tau &= (10, 10, 8, 8, 8, 7, 6, 6, 6, 5, 2). \end{aligned} \tag{3}$$

For the skew shape  $\lambda/\mu$ , choose fixed shift 2, and for the skew shape  $\sigma/\tau$  choose fixed shift 0, and consider the starting and ending points of the corresponding families of nonintersecting lattice paths. For instance, the ending point of the first path corresponding to  $\lambda/\mu$  is  $(\lambda_1 - 1 + 2, N) = (15, N)$ , and the starting point of the last (twelfth) path corresponding to  $\lambda/\mu$  is  $(\mu_{12} - 12 + 2, 1) = (-10, 1)$ , and the ending point of the first path corresponding to  $\sigma/\tau$  is  $(\sigma_1 - 1, N) = (13, N)$ .

Now colour the starting/ending points corresponding to  $\lambda/\mu$  *white*, and the starting/ending points corresponding to  $\sigma/\tau$  *black*: See the upper picture of Figure 2, where

the starting/ending points of  $\lambda/\mu$  are drawn as white circles, and the starting/ending points of  $\sigma/\tau$  are drawn as black circles.

All starting/ending points which are coloured both black *and* white are never affected by the following constructions: In the upper picture of Figure 2, these points are enclosed by grey rectangles.

We call the remaining starting/ending points (which are coloured *either* black *or* white) the *coloured* points. Note that the number of coloured points is necessarily *even*.

For the coloured points, assume the circular orientation “from right to left along level  $N$ , and then from left to right along level 1”. In the upper picture of Figure 2, this circular orientation is indicated by a grey circular arrow.

Furthermore, assign to paths corresponding to  $\lambda/\mu$  the orientation *downwards*, and to paths corresponding to  $\sigma/\tau$  the orientation *upwards*. In the upper picture of Figure 2, this orientation of paths is indicated by upwards or downwards pointing triangles.

If we focus on the coloured points, we may encode the situation in a simpler picture, where the coloured starting/ending points are located on the lower/upper half of a *circle*, and where the orientation of the respective path is translated to a *radial orientation* (either towards the center of the circle or away from it). The lower picture of Figure 2 illustrates this: A grey horizontal line indicates the separation of the lower and upper half of the circle, the point labeled 1 corresponds to the lattice point  $(15, N)$ , the point labeled 2 corresponds to the lattice point  $(6, N)$ , and so on.

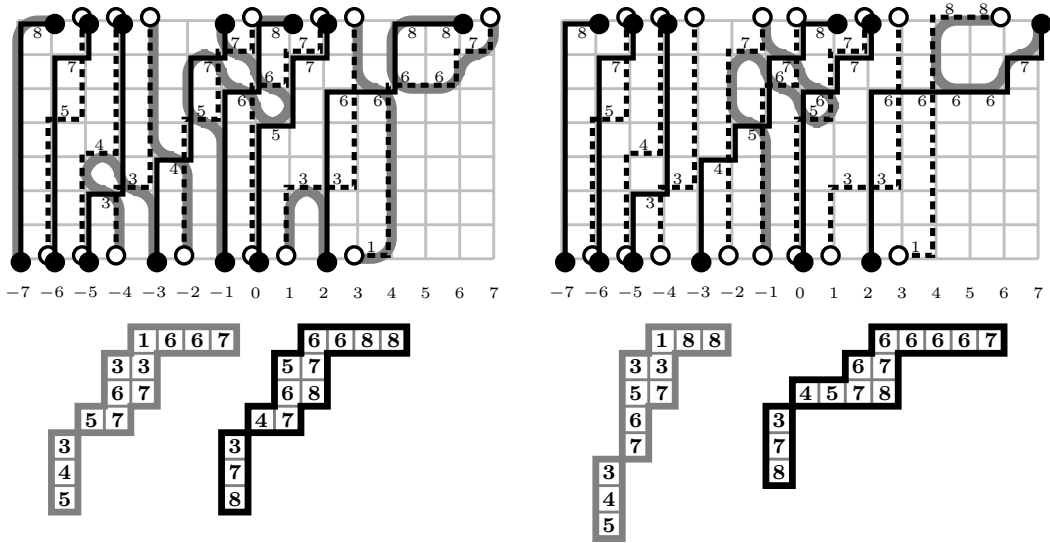
Now consider some pair  $(P_1, P_2)$  of families of nonintersecting lattice paths, where  $P_1$  corresponds to some tableau of shape  $\lambda/\mu$ , and  $P_2$  corresponds to some tableau of shape  $\sigma/\tau$ . We call the paths of  $P_1$  the *white* paths and the paths of  $P_2$  the *black* paths, and we colour the arcs of the lattice  $\mathbb{Z}^2$  accordingly (i.e., arcs used by some white path are coloured white, and arcs used by some black path are coloured black). As with the starting/ending points, arcs which are coloured black *and* white are not affected by the following construction, and we call all arcs which are *either* black *or* white the *coloured* arcs. We construct *bicoloured paths*

- connecting (only) coloured starting/ending points
- and using (only) coloured arcs

by the following algorithm:

We start at some coloured point  $q$  and follow the path determined by the *unique* coloured arc incident with it in the respective orientation (i.e., either up/right or down/left). Whenever we meet *another* path on our way (necessarily, this path is of the other colour), we “change colour and orientation”, i.e., we follow this new path *and* change the orientation (i.e., if we were moving up/right along the old path, we move down/left along the new path, and vice versa). We stop if there is no possibility to go further.

FIGURE 3. The left picture presents two tableaux of the identical shape  $(7, 4, 4, 3, 1, 1, 1) / (3, 2, 2, 1)$  in the lower part, the upper part shows the corresponding overlay of black and white paths (white paths are indicated by dashed lines) and *all* bicoloured paths (indicated by thick grey lines). The right picture presents two tableaux of shapes  $(5, 3, 3, 2, 2, 1, 1, 1) / (2, 1, 1, 1, 1)$  and  $(9, 5, 5, 1, 1, 1) / (4, 3, 1)$ , respectively, in the lower part: These tableaux correspond to the overlay of lattice paths in the upper part, which is obtained by *recolouring* the bicoloured paths starting in  $(7, 8)$  and in  $(-1, 1)$  (these bicoloured paths are indicated by thick grey lines, again).



This construction is described in detail in [1]. Here, we simply refer to the left picture of Figure 3, where the white paths are indicated by dashed lines, and all bicoloured paths are indicated by thick grey lines.

The following observations are immediate:

**Observation 1 (Bicoloured paths always exist).** For *every* coloured point  $q$ , there exists a bicoloured path starting at  $q$ .

**Observation 2 (Bicoloured paths connect points of different radial orientation).** The bicoloured paths thus constructed never connect points of the same radial orientation (i.e., two points oriented both towards or both away from the center).

In the lower picture of Figure 2, a possible pattern of “connections by bicoloured paths” is indicated by dashed lines.

The following observation is easy to see:

**Observation 3 (Bicoloured path connect points of different parity).** Two different bicoloured paths may have lattice points in common (they may intersect), but they can never *cross*. If we assume some consecutive numbering of the coloured points in their circular orientation (see the lower picture of Figure 2), then this non-crossing condition

implies that there can never be a bicoloured path connecting two points with numbers of the same parity.

The non-crossing condition means that if all such connections were drawn as straight lines connecting points on the circle, then no two such lines can intersect. (In Figure 2, not all connections are drawn as straight lines for graphical reasons.)

Consider some bicoloured path  $b$  in the overlay of nonintersecting lattice paths  $(P_1, P_2)$ : Changing colours (black to white and vice versa)

- of both ending points of  $b$
- and of all arcs of  $b$

gives a new overlay of nonintersecting lattice paths  $(P'_1, P'_2)$  (with different starting/ending points). It is easy to see that we have for this *recolouring* of a bicoloured path:

**Observation 4 (Recolouring bicoloured paths is a weight preserving involution).** The recolouring of a bicoloured path  $b$  in an overlay of nonintersecting lattice paths  $(P_1, P_2)$  is an *involution operation* (i.e., if we obtain the overlay  $(P'_1, P'_2)$  by recolouring  $b$  in  $(P_1, P_2)$ , then recolouring  $b$  again in  $(P'_1, P'_2)$  yields the original  $(P_1, P_2)$ ), which *preserves the respective weights*, i.e.,

$$\omega(P_1) \cdot \omega(P_2) = \omega(P'_1) \cdot \omega(P'_2).$$

Return to the example illustrated in Figure 2 and consider the white ending point  $(15, N)$  and the black starting point  $(5, 1)$  there. Note that both of these points are marked with a triangle pointing *downward*. The bicoloured paths ending at these points must have their other ending points marked with a triangle pointing *upward*. One possible choice of these other ending points is depicted in Figure 4: The corresponding ending points are marked by white rectangles, the bicoloured paths are indicated by arrows. The picture shows the situation *after* recolouring these paths.

The skew shape corresponding to the white points in Figure 4 is  $\lambda'/\mu'$ , where

$$\begin{aligned} \lambda' &= (13, 13, 11, 11, 9, 9, 8, 8, 7, 5, 3), \\ \mu' &= (9, 9, 7, 7, 7, 6, 5, 5, 5, 4, 0). \end{aligned} \tag{4}$$

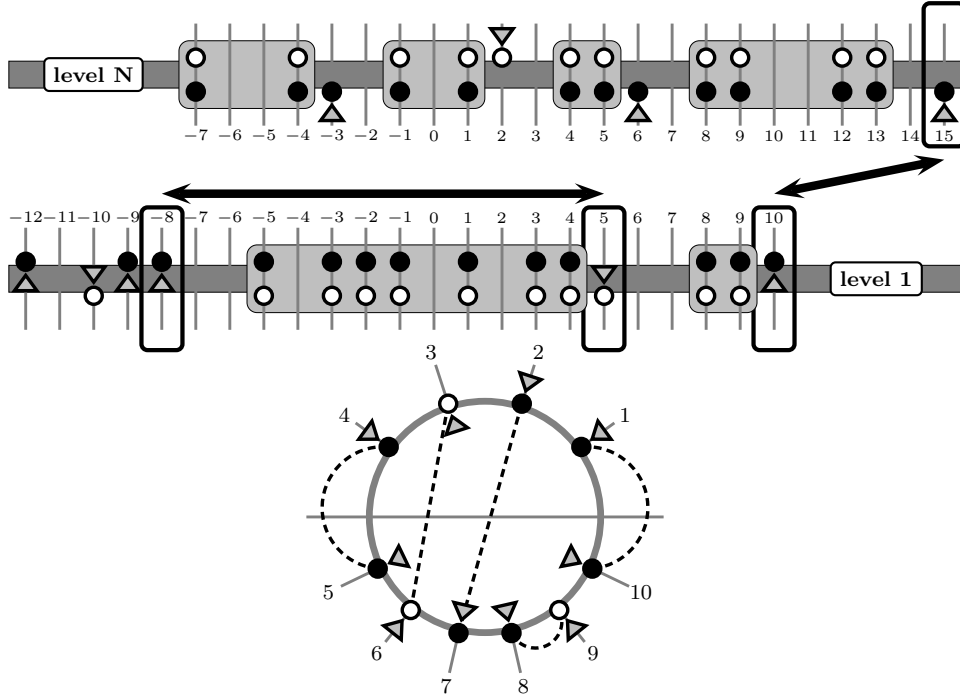
The skew shape corresponding to the black points in Figure 4 is  $\sigma'/\tau'$ , where

$$\begin{aligned} \sigma' &= (15, 14, 14, 12, 12, 11, 11, 11, 9, 8, 7, 7, 5), \\ \tau' &= (10, 10, 10, 7, 7, 6, 5, 5, 5, 4, 2, 2, 0). \end{aligned} \tag{5}$$

For both skew shapes, the starting and ending points are shifted by 1, so, for instance, the starting point of the first path corresponding to  $\sigma'/\tau'$  is  $(\tau'_1 - 1 + 1, 1) = (10, 1)$  and the ending point of the last (eleventh) path corresponding to  $\lambda'/\mu'$  is  $(\lambda'_{11} - 11 + 1, N) = (-7, N)$ .

The pictures in Figure 4 contain redundant information: All uncoloured points are “doubled”, and the colour (black or white) of the coloured points is determined uniquely by their circular orientation. So we may encode the information in a more terse way, namely as

FIGURE 4. The two (necessarily different, by Observation 2!) bicoloured paths in Figure 2 which start at the white ending point  $(15, N)$  and at the the black starting point  $(5, 1)$  may have their respective other ending points in  $(10, 1)$  and  $(-8, 1)$ . In the picture below, the corresponding points are marked by white rectangles, the bicoloured paths are indicated by arrows. The picture shows the situation *after* recolouring these paths.



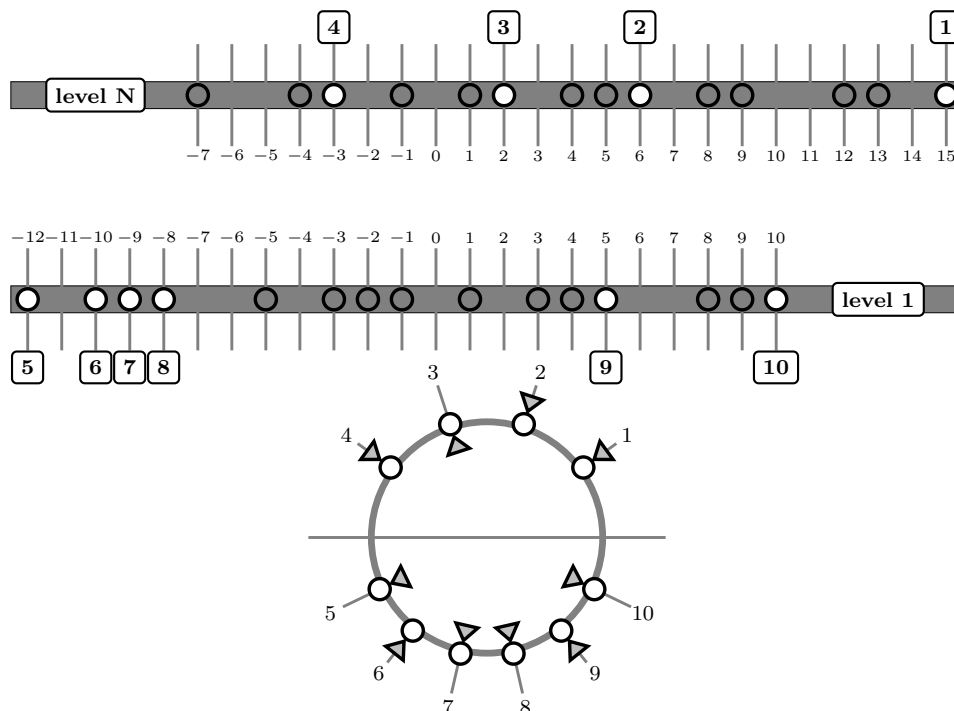
- the *configuration of (starting/ending) points* (short: **cp**) (see the upper picture in Figure 5),
- and the *circular orientation of coloured (starting/ending) points* (short: **cocp**) (see the lower picture in Figure 5).

We call a **cocp** *admissible* if it has the same number of inwardly/outwardly oriented points. *Every* admissible **cocp** determines (together with the corresponding **cp**) a certain configuration of starting/ending points. However, there might be no overlay of families of nonintersecting lattice paths that connect these points (if, for instance, the  $i$ -th white ending point lies to the left of the  $i$ -th white starting point; this would correspond to an  $i$ -th row of length  $< 0$  in the corresponding shape): In this case, the corresponding skew Schur function is zero. But if there *is* an overlay of families of nonintersecting lattice paths that connect these points, then the family of all bicoloured paths determines a *perfect matching*  $M$  in the **cocp** (according to Observation 1), which is *non-crossing* (according to Observation 3), and where all edges of  $M$  connect points of different radial orientation (according to Observation 2): We call such matchings *admissible*. Note that recolouring some bicoloured path amounts to reversing the orientation of the corresponding edge in the matching  $M$ .

We may summarize all these considerations as follows (this is a reformulation of [1, Lemma 15]):



FIGURE 5. The information of Figure 4 can be encoded in a more terse way, namely as the **cp** (shown in the upper picture) and the **cocp** (shown in the lower picture): The grey points in the upper picture are “doubled” points (coloured black *and* white), and the colour of the white points in the upper picture is determined by the *orientation* of the corresponding points in the lower picture (points in the upper half which are inwardly orientated and points in the lower half which are outwardly oriented should be coloured black; all other points should be coloured white).



**Lemma 1.** *Let  $\lambda/\mu$  and  $\sigma/\tau$  be two skew shapes, and let  $t$  be an arbitrary integer. Consider the **cp** corresponding to the starting/ending points with shift 0 for  $\lambda/\mu$  and shift  $t$  for  $\sigma/\tau$ . In the corresponding **cocp**, choose a nonempty subset  $S$  (arbitrary, but fixed) of the points oriented towards the center.*

*Consider the set  $V$  of all admissible **cocps**, and consider the graph  $G$  with vertex set  $V$ , where two vertices  $v_1, v_2$  are connected by an edge if and only if there are overlays of lattice paths  $(P_1, P_2)$  and  $(P'_1, P'_2)$  for the starting/ending points corresponding to  $(\mathbf{cp}, v_1)$  and  $(\mathbf{cp}, v_2)$ , respectively, such that  $(P'_1, P'_2)$  is obtained from  $(P_1, P_2)$  by recolouring all bicoloured paths that are incident with some point of  $S$ .*

*Obviously, this graph  $G$  is bipartite (i.e.,  $V = E \cup O$  with  $E \cap O = \emptyset$ , such that there is no edge connecting two vertices of  $E$  or two vertices of  $O$ ).*

*Let  $C$  be an arbitrary connected component of  $G$  with at least 2 vertices, and denote by  $C_O$  the set of pairs of skew shapes corresponding to  $(\mathbf{cp}, x)$  for  $x \in O$ , and by  $C_E$  the set of pairs of skew shapes corresponding to  $(\mathbf{cp}, x)$  for  $x \in E$ . Then we have the following*

identity for skew Schur functions:

$$\sum_{(\lambda/\mu, \sigma/\tau) \in C_E} s_{\lambda/\mu} \cdot s_{\sigma/\tau} = \sum_{(\lambda'/\mu', \sigma'/\tau') \in C_O} s_{\lambda'/\mu'} \cdot s_{\sigma'/\tau'}. \quad (6)$$

This Lemma is rather unwieldy. But there is a particularly simple situation which appears to be useful, so we state it as a Theorem (this is a reformulation of [1, Lemma 16]):

**Theorem 1.** *Under the assumptions of Lemma 1, let  $c$  be the **cocp** for the pair of shapes  $(\lambda/\mu, \sigma/\tau)$ , and assume that the orientation of the points in  $c$  is alternating. As in Lemma 1, let  $S$  be some fixed subset of the points oriented towards the center in  $c$ .*

*Consider the set of all **cocps** which can be obtained by reorienting all edges incident with points in  $S$  in some admissible matching of  $c$ , and denote the set of pairs of skew shapes corresponding to such **cocps** by  $Q$ .*

Then we have:

$$s_{\lambda/\mu} \cdot s_{\sigma/\tau} = \sum_{(\lambda'/\mu', \sigma'/\tau') \in Q} s_{\lambda'/\mu'} \cdot s_{\sigma'/\tau'}. \quad (7)$$

*Proof.* Observe that in the right hand side of (7) the Schur function product  $s_{\lambda'/\mu'} \cdot s_{\sigma'/\tau'}$  is either zero (if there is, in fact, no overlay of families of nonintersecting lattice paths corresponding to the respective **cocp**), or there is some corresponding overlay of families of nonintersecting lattice paths  $(P'_1, P'_2)$ . In the latter case, there *are* bicoloured paths starting in the points of  $S$  (by Observation 1), and by the combination of Observations 2 and 3, recolouring all such paths necessarily yields an overlay  $(P_1, P_2)$  of nonintersecting lattice paths which corresponds to the pair  $(\lambda/\mu, \sigma/\tau)$ .  $\square$

#### 4. APPLICATIONS

Clearly, the interpretation of Schur functions as generating functions of  $r$ -tuples of nonintersecting lattice paths is best suited for the bijective construction of recolouring bicoloured paths. But of course, the recolouring operation can be translated into operations for the shapes of the corresponding tableau (i.e., for the corresponding partitions, or equivalently, Ferrers diagrams).

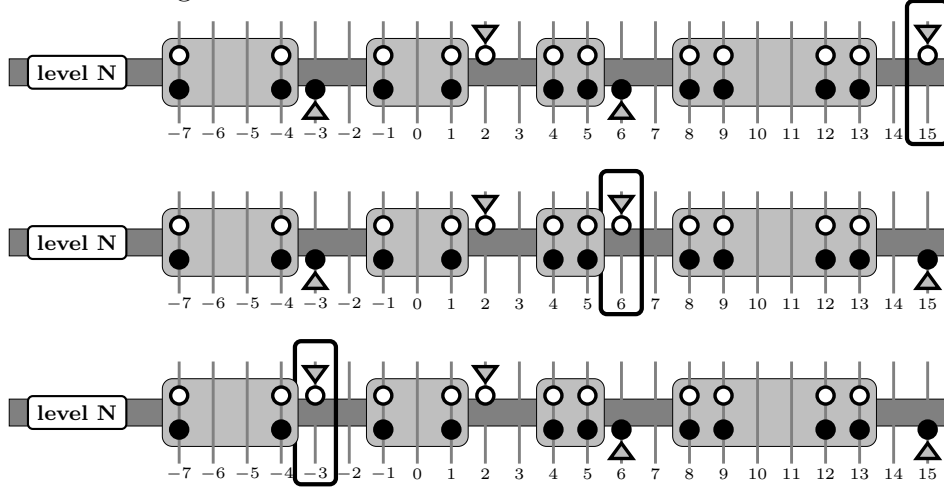
We shall show how this translation gives the identity [4, (3.3)] of Gurevich, Pyatov and Saponov, but before doing this we consider a simple special case, in order to illustrate the meaning of Theorem 1:

**Example 1.** *Assume that for the shapes  $\lambda/\mu$  and  $\sigma/\tau$  we have*

- $\mu = \tau$ ,
- $\lambda_1 > \sigma_1$ ,
- $\ell(\lambda) = \ell(\sigma)$ .

*Choose shift 0 for the families of starting/ending points corresponding to these shapes, then there is no coloured starting point (since  $\mu = \tau$ ): accordingly, only the ending points are shown in Figure 6. Furthermore, assume that the corresponding black and white ending points alternate along level  $N$ : Then the preconditions of Theorem 1 are fulfilled.*

FIGURE 6. Application of Lemma 1 to the special case  $\mu = \tau$ ,  $\lambda_1 > \sigma_1$ ,  $\ell(\lambda) = \ell(\sigma)$ , and shift 0 for *all* starting/ending points: Since there is no coloured starting point in this case, only the ending points (on level  $N$ ) are shown. The point  $(15, N)$  (ending point of bicoloured path  $b$ ) is marked with a white rectangle in the upper row. The middle row and the lower row show the configurations which can arise by recolouring  $b$ ; the respective other ending points  $(6, N)$  and  $(-3, N)$  are again marked with a white rectangle.



Since  $\lambda_1 > \mu_1$ , the point  $q = (\lambda_1 - 1, N)$  is white. Consider the set  $S = \{q\}$ : The bicoloured path  $b$  starting in  $q$  necessarily end in a black point (by Observation 2). Assume that there are  $k$  such black points  $q_1, \dots, q_n$ , and let  $\lambda^{(i)}$  and  $\sigma^{(i)}$  be the partitions corresponding to the configuration of white and black points obtained by changing colours of  $q$  and  $q_i$ ,  $i = 1, \dots, k$  (i.e., colour  $q$  black and  $q_i$  white, and leave all other colours unchanged). Then by Theorem 1 we have:

$$s_{\lambda/\mu} \cdot s_{\sigma/\mu} = \sum_{i=1}^k s_{\lambda^{(i)}/\mu} \cdot s_{\sigma^{(i)}/\mu}$$

Figure 6 illustrates this example for

$$\begin{aligned} \lambda &= (16, 15, 15, 13, 13, 11, 11, 10, 10, 9, 7, 5), \\ \sigma &= (14, 14, 12, 12, 11, 11, 11, 9, 8, 7, 7, 5). \end{aligned}$$

From the pictures in Figure 6 we see that  $k = 2$  in this case, with

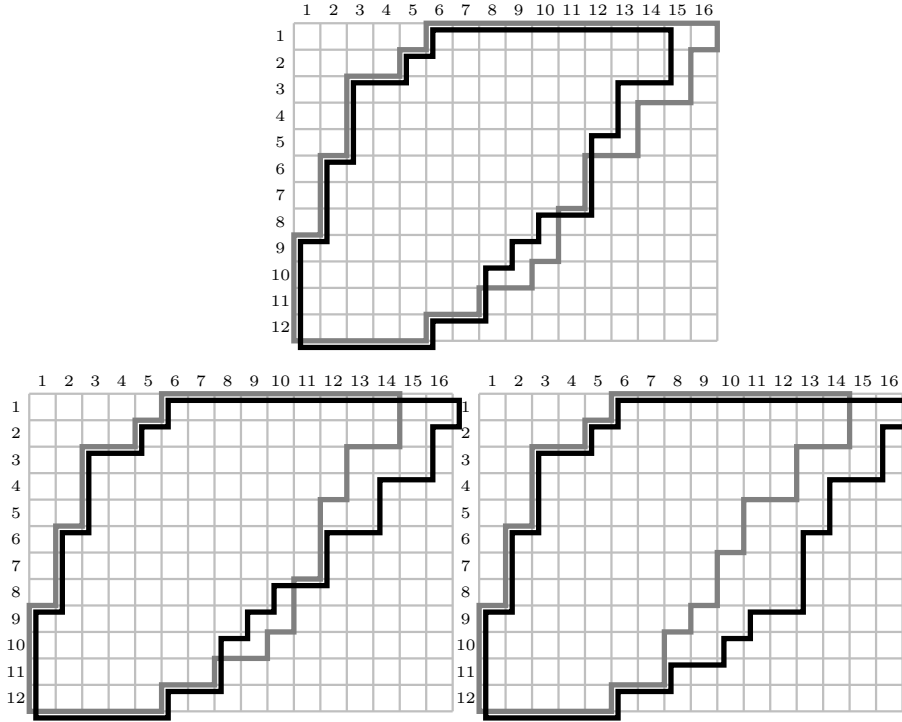
$$\begin{aligned} \lambda^{(1)} &= (14, 14, 12, 12, 11, 11, 11, 10, 10, 9, 7, 5), \\ \sigma^{(1)} &= (16, 15, 15, 13, 13, 11, 11, 9, 8, 7, 7, 5), \end{aligned}$$

(shown in the middle row of Figure 6) and

$$\begin{aligned} \lambda^{(2)} &= (14, 14, 12, 12, 10, 10, 9, 9, 8, 7, 7, 5), \\ \sigma^{(2)} &= (16, 15, 15, 13, 13, 12, 12, 12, 10, 9, 7, 5) \end{aligned}$$

(shown in the lower row of Figure 6). Figure 7 presents the Ferrers diagrams for this example, where we chose  $\mu = \tau = (5, 4, 2, 2, 1, 1, 1)$ .

FIGURE 7. The skew Ferrers boards corresponding to the example in Figure 6 for  $\mu = \tau = (5, 4, 2, 2, 2, 1, 1, 1)$ : The upper picture shows the Ferrers board of  $\lambda/\mu$  (drawn with grey lines) and  $\sigma/\tau$  (drawn with black lines). The lower pictures show the Ferrers boards of  $\lambda^{(i)}/\mu$  and  $\sigma^{(i)}/\tau$ ,  $i = 1, 2$ .



**4.1. The identity of Gurevich, Pyatov and Saponov.** Now consider the special case  $\mu = \tau$ ,  $\lambda_1 > \sigma_1$ ,  $\ell(\lambda) = \ell(\sigma) + 1$ , with shift 0 for all starting and ending points, and where black and white points alternate in their circular orientation. As in Example 1, let  $q = (\lambda_1 - 1, N)$  and choose  $S = \{q\}$ . The possible ending points of the bicoloured path  $b$  ending in  $q$  are

- the black points at level  $N$
- and the leftmost white starting point  $q_0$ .

As our running example we choose the skew shapes  $\lambda/\mu$  and  $\sigma/\tau$  with

$$\begin{aligned}\lambda &= (10, 7, 7, 6, 6, 4, 4, 3, 2, 2), \\ \sigma &= (8, 7, 7, 5, 4, 4, 2, 1, 1), \\ \mu = \tau &= (4, 3, 3, 1).\end{aligned}$$

See the upper picture in Figure 8 for an illustration.

Assume that there are  $k > 1$  black points  $q_1, \dots, q_k$  and denote the shapes corresponding to recolouring  $q$  and  $q_i$ ,  $i = 0, 1, \dots, k$ , by  $\lambda^{(i)}/\mu$  and  $\sigma^{(i)}/\mu$ , respectively. Then by

FIGURE 8. Application of Theorem 1 to the special case  $\mu = \tau$ ,  $\lambda_1 > \sigma_1$ ,  $\ell(\lambda) = \ell(\sigma) + 1$  and shift 0 for all starting and ending points: Consider the configurations that can arise by recolouring the bicoloured path  $b$  ending in  $q = (\lambda_1 - 1, N)$ . The uppermost picture shows the configuration of the starting and ending points of  $\lambda/\mu$  (drawn as white circles) and  $\sigma/\tau$  (drawn as black circles), where  $\mu = \tau = (4, 3, 3, 1)$ . The point  $q = (\lambda_1 - 1, N)$  is marked by a white rectangle.

The three pictures below show the three possible configurations arising by the recolouring of  $b$ ; the other ending point of  $b$  is marked by a white rectangle.

From Theorem 1 we obtain the Schur function identity

$$s_{\lambda/\mu} \cdot s_{\sigma/\tau} = s_{\lambda^{(0)}/\mu} \cdot s_{\sigma^{(0)}/\mu} + s_{\lambda^{(1)}/\mu} \cdot s_{\sigma^{(1)}/\mu} + s_{\lambda^{(2)}/\mu} \cdot s_{\sigma^{(2)}/\mu}.$$

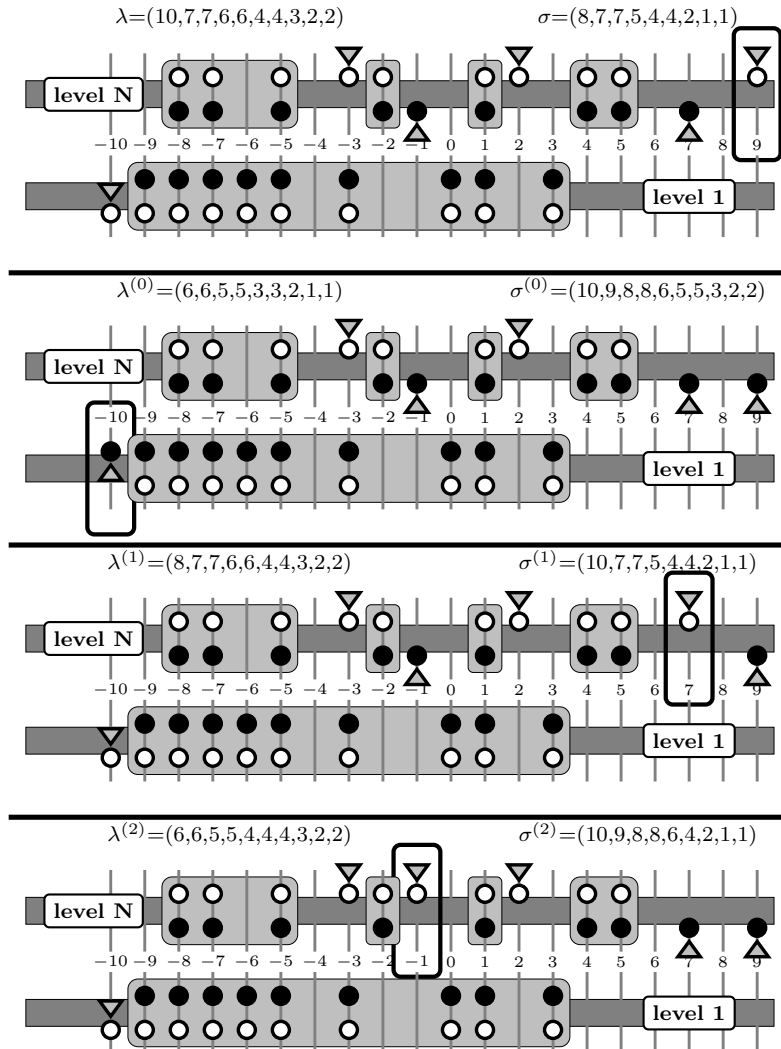
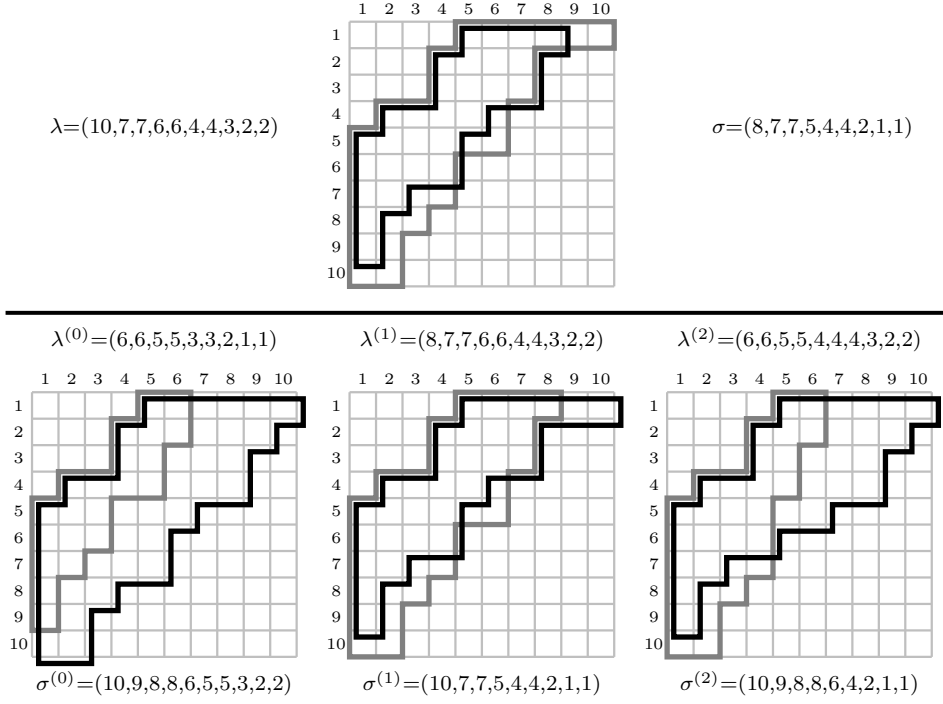


FIGURE 9. The skew Ferrers diagrams corresponding to the example in Figure 8: The upper picture shows the overlay of the Ferrers diagrams for  $\lambda/\mu$  and  $\sigma/\mu$  (without recolouring), and the lower pictures show the overlay of diagrams  $\lambda^{(i)}/\mu$  and  $\sigma^{(i)}/\mu$ ,  $i = 0, 1, 2$ .



Theorem 1 we have:

$$s_{\lambda/\mu} \cdot s_{\sigma/\mu} = s_{\lambda^{(0)}/\mu} \cdot s_{\sigma^{(0)}/\mu} + \sum_{i=1}^k s_{\lambda^{(i)}/\mu} \cdot s_{\sigma^{(i)}/\mu} \quad (8)$$

See the three lower pictures in Figure 8 for an illustration (in this example,  $k = 2$ ).

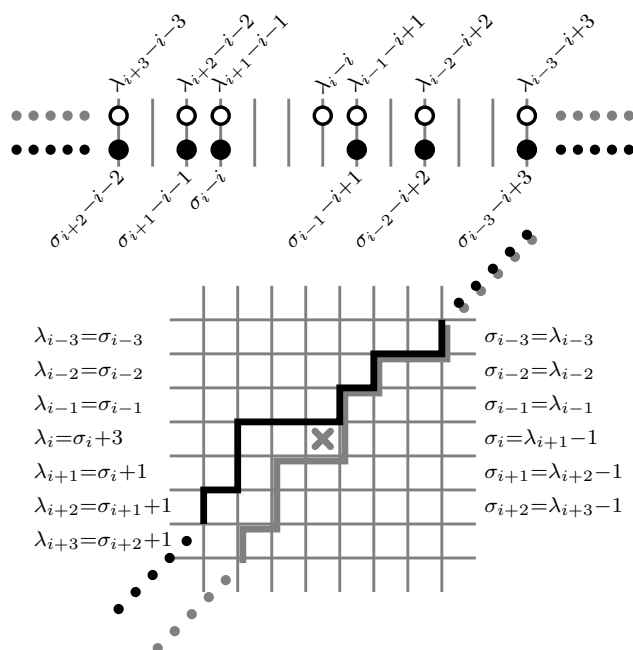
If we choose  $\mu = 0$ , (8) amounts precisely to the identity [4, (3.3)]: We simply have to *translate* our formulation to the language of adding and removing *partial border strips* to Ferrers diagrams, which was used by Gurevich, Pyatov and Saponov [4]. To get a first idea, have a look at Figure 9, which presents the Ferrers diagrams corresponding to the concrete example of Figure 8.

Observe that recolouring starting/ending points may be viewed as a game of inserting/removing points in the configuration of starting/ending points corresponding to some partition. Instead of giving a lengthy verbal description, we present in Figure 10 the effect of inserting (read the upper picture upwards, from  $\sigma$  to  $\lambda$ ) or removing (read the upper picture downwards, from  $\lambda$  to  $\sigma$ ) points in a graphical way.

Reading the upper part of Figure 10 *downwards* (i.e., removing the point in position  $\lambda_i - i$ ), the Ferrers diagram of  $\sigma$  is obtained from the Ferrers diagram of  $\lambda$  by a *down-peeling* of a *partial border strip* starting at row  $i$ , or, in the language of [4]:

$$\sigma = \lambda \downarrow^i.$$

FIGURE 10. The operation of inserting/removing points in the configuration of starting/ending points can be translated to the language introduced in [4], i.e., to operations on Ferrers diagrams: In the lower part of the picture, the grey lines correspond to the Ferrers diagram of  $\lambda$ , and the black lines correspond to the Ferrers diagram of  $\sigma$ . Reading the upper part of the picture *downwards* (i.e., removing the point in position  $\lambda_i - i$ ), the Ferrers diagram of  $\sigma$  is obtained from the Ferrers diagram of  $\lambda$  by a *down-peeling* of a *partial border strip* starting at row  $i$ :  $\sigma = \lambda \downarrow^i$ . The partial border strip is the area between the black and grey shapes in rows  $i, i + 1, \dots$ : It is clear that such strip begins with the last box in row  $i$  (indicated by a grey "x" in the picture).



The special case of this operation for  $i = 1$  amounts to the removal of the *complete* border strip — in the language of [4]:

$$\lambda \downarrow := \lambda \downarrow^1.$$

Now observe that a pair of partitions  $(\lambda, \sigma)$  fulfilling the preconditions for (8) can be obtained by *constructing* an appropriate  $\sigma$  for a given  $\lambda$ . This is achieved by applying to the configuration of ending points corresponding to  $\lambda$  a sequence of  $k$  removals/insertions of points, followed by removing the right-most ending point and inserting a new left-most starting point, see the upper picture in Figure 8.

Again, we shall illustrate the simple procedure by pictures instead of giving a lengthy verbal description.

The first step of this construction is illustrated in Figure 11: The configuration of points corresponding to the partition  $\lambda = (10, 7, 7, 6, 6, 4, 4, 3, 2, 2)$  considered in Figure 8 is presented in the upper part of the picture. This configuration is changed by adding a

new point at position 7 first (the result of this change is presented in the middle part of the picture) and then by removing the point at position 2 (the result of this change is presented in the lower part of the picture). It is obvious that this amounts to adding a *partial border strip* to the Ferrers diagram of  $\lambda$ , which consists of  $t_1 = 2$  boxes in row  $r_1 = 2$  and spans the  $m_1 = 3$  rows 2, 3 and 4. Stated in the language introduced in [4], the picture in the lower row of Figure 11 shows

$$\lambda +_{(r_1, m_1)}^{t_1}.$$

The next step of this construction is to add a point at position  $-1$  and to remove the point at position  $-3$ . This amounts to adding a partial border strip consisting of  $t_2 = 2$  boxes in row  $r_2 = 6$  and spanning the  $m_2 = 2$  rows 6 and 7. We thus obtain  $\nu = (10, 9, 8, 8, 6, 5, 5, 3, 2, 2)$ , or, in the language of [4]:  $\nu = \lambda +_{(2,3),(6,2)}^{2,1}$ , see the upper picture in Figure 12.

Finally, we remove the rightmost ending point at position 9: This amounts to removing a *complete* border strip from the Ferrers diagram of  $\nu$ , giving the partition  $\sigma = \nu \downarrow = (8, 7, 7, 5, 4, 4, 2, 1, 1)$  of our running example, see the lower picture in Figure 12.

So we see that the Schur function identity stated in Figure 8 can be partially translated as:

$$s_{\lambda/\mu} \cdot s_{\nu \downarrow / \tau} = s_{\lambda \downarrow / \mu} \cdot s_{\nu / \mu} + \dots$$

To complete this translation, have a look at Figure 13 and note that the partitions  $\lambda^{(1)}$  and  $\lambda^{(2)}$  (drawn with black lines) are obtained by the original partition  $\lambda$  (drawn with grey lines) by removing a partial border strip which starts in the box marked with a small “x” and extends up to the first row. Note that for such *up-peeling* of a border strip starting at row  $i$ , there are  $\lambda_i - \lambda_{i+1}$  possible positions of the starting box: Number them from left to right, then the up-peeling is uniquely determined by the row number  $i$  and the box number  $t$ . In the language of [4], this is denoted by

$$\lambda \uparrow_{(i,t)},$$

i.e., we have  $\lambda^{(1)} = \lambda \uparrow_{(1,2)}$  and  $\lambda^{(2)} = \lambda \uparrow_{(5,1)}$ .

Putting all these observations together, we see that the Schur function identity stated in Figure 8 can be translated as:

$$s_{\lambda/\mu} \cdot s_{\nu \downarrow / \tau} = s_{\lambda \downarrow / \mu} \cdot s_{\nu / \mu} + s_{\lambda \uparrow_{(1,2)} / \mu} \cdot s_{\nu \downarrow^2 / \mu} + s_{\lambda \uparrow_{(5,1)} / \mu} \cdot s_{\nu \downarrow^6 / \mu}.$$

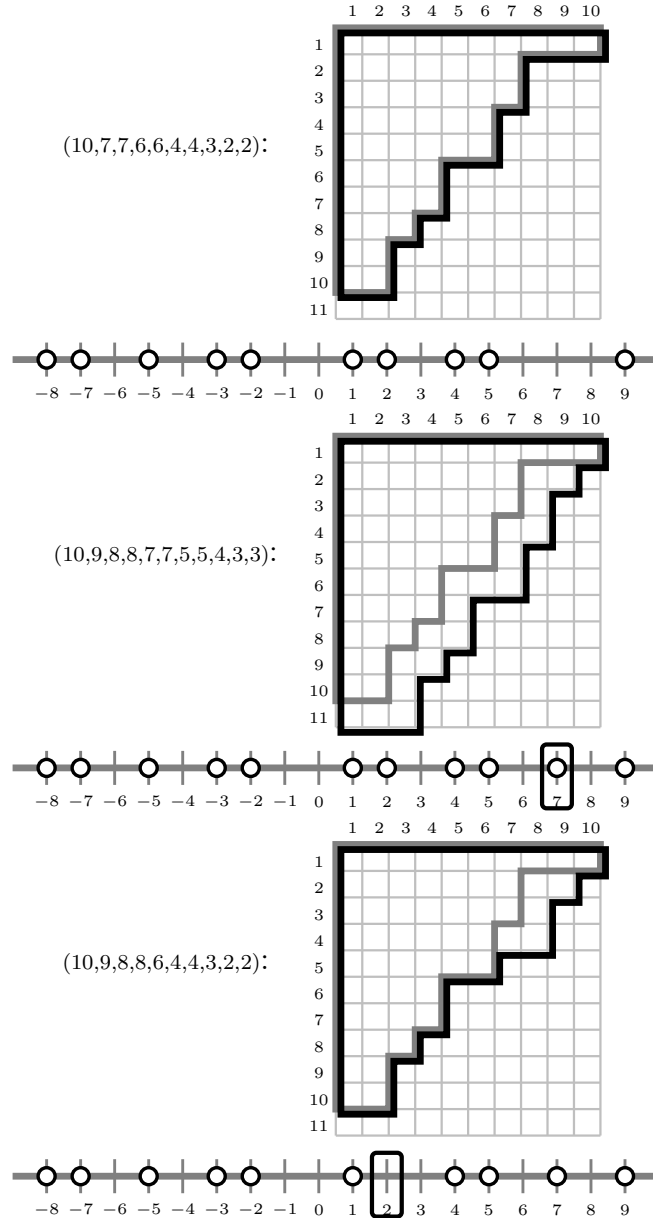
So it is clear that the special case considered in this section can be stated as follows:

**Corollary 1** (Gurevich, Pyatov and Saponov). *Let  $\lambda = (\lambda_1, \dots, \lambda_r)$  be a partition. Assume that there are  $k$  indices  $2 \leq r_1 < \dots < r_k \leq r$  such that  $\lambda_{r_i} < \lambda_{r_{i-1}}$ ,  $i = 1, \dots, k$ . Choose integers  $t_i$  and  $m_i$  for  $i = 1, \dots, k$  subject to the restrictions*

$$\begin{aligned} 1 &\leq t_i \leq \lambda_{r_{i-1}} - \lambda_{r_i}, \\ 1 &\leq m_i \leq r_{i+1} - r_i. \end{aligned}$$



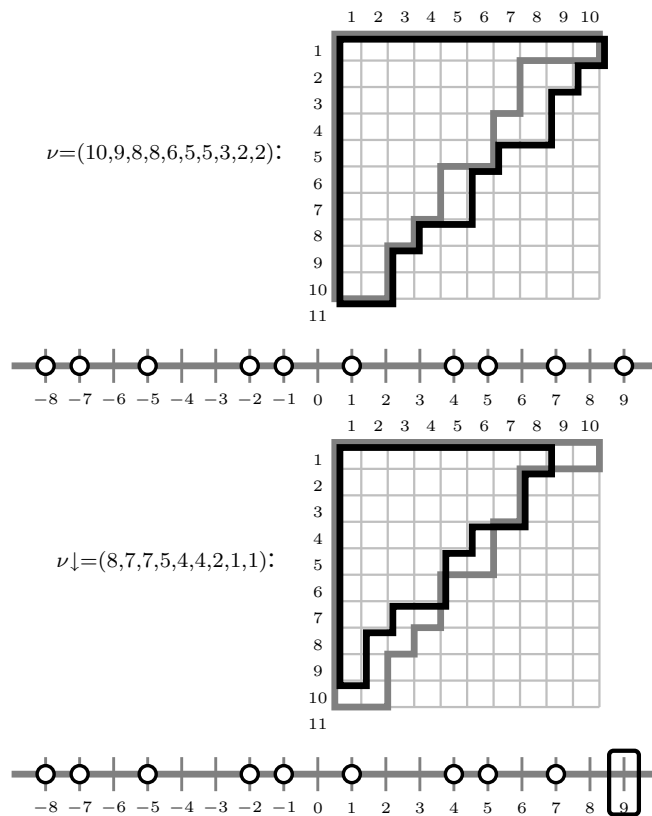
FIGURE 11. Adding some point at position  $i$  and removing a point at position  $j < i$  amounts to adding a *partial border strip*. The pictures show the Ferrers diagram of the original partition  $\lambda$  with grey lines, and the Ferrers diagrams of the partitions obtained by adding/removing points with black lines. The corresponding configuration of ending points is depicted under the Ferrers diagrams.



Then we may construct  $\nu = \lambda \uparrow_{(r_1, m_1) \dots (r_k, m_k)}^{t_1, \dots, t_k}$ , and we have

$$s_\lambda \cdot s_{\nu \downarrow} = s_{\lambda \downarrow} \cdot s_\nu + \sum_{i=1}^k s_{\lambda \uparrow_{(r_i-1, t_i)}} \cdot s_{\nu \downarrow_{(r_i)}}$$

FIGURE 12. Removing the point corresponding to  $\nu_1$  (marked by a white rectangle in the lower picture) amounts to removing the *complete border strip* spanning rows 1, 2,  $\dots$ ,  $\ell(\nu)$  from the Ferrers board of  $\nu$ , see Figure 10.



## REFERENCES

- [1] Markus Fulmek and Michael Kleber. Bijective proofs for Schur function identities which imply Dodgson's condensation formula and Plücker relations. *Electron. J. Combin.*, 8(1):Research Paper 16, 22 pp. (electronic), 2001.
- [2] Ira M. Gessel and Xavier Viennot. Determinants, paths, and plane partitions. preprint, 1998.
- [3] Ian P. Goulden. Quadratic forms of skew Schur functions. *European J. of Combinatorics*, 9:161–168, 1988.
- [4] Dimitri Gurevich, Pavel Pyatov, and Pavel Saponov. Bilinear identities on Schur symmetric functions. arXiv:0907.4292v1 [math.CO].
- [5] Bruce E. Sagan. *The Symmetric Group*. Springer, 2nd edition, 2000.

FAKULTÄT FÜR MATHEMATIK, NORDBERGSTRASSE 15, A-1090 WIEN, AUSTRIA

*E-mail address:* Markus.Fulmek@Univie.Ac.At

*WWW:* <http://www.mat.univie.ac.at/~mfulmek>

FIGURE 13. Removing the point corresponding to  $\lambda_1$  and inserting a new point at positions 7 and  $-1$ , respectively (these points are marked by white rectangles in the pictures) yield the partitions  $\lambda^{(1)}$  and  $\lambda^{(2)}$  from Figure 8, respectively. In the language of [4],  $\lambda^{(1)}$  is obtained by the *up-peeling* of a partial border strip starting in row 1 at the second possible box (marked by a grey “x” in the upper picture), and  $\lambda^{(2)}$  is obtained by the up-peeling of a partial border strip starting in row 5 at the first possible box (marked by a grey “x” in the upper picture):  $\lambda^{(1)} = \lambda \uparrow_{(1,2)}$  and  $\lambda^{(2)} = \lambda \uparrow_{(5,1)}$ .

